A three-layer groundwater model is presented to explore the use of multiple beta associations, anisotropy, and a larger number of parameters. In this case, the model is 40 rows by 35 columns across 3 layers. The row spacing is 2.0 meters (m) while the column spacing is 1.5 m. The layers, from shallowest to deepest, are 1.8 m, 1.4 m, and 1.8 m in thickness, respectively. The disparate row, column, and layer spacing was used to test the Toeplitz compression option. The model has constant head boundaries on all sides (set at the same elevation—60 m) and a single well at row 18, column 17, extracting at 0.01 liters per minute from each layer. This low flow rate is not meant to represent typical field conditions, but rather highlights what can be learned with even a very small stress on the system.

The true parameter field, shown in figure 6.1, varies from 0.01 to 0.075 meter per day.

Five cases are illustrated here, as summarized in table 6.1. In all cases, each layer is treated as a separate beta association. In each of these layers, the initial value for the prior structural parameter (the linear variogram slope, θ) is 1.0×10^{-5}.

Cases 1 and 2 illustrate how the level of fit (and, therefore, the degree of roughness of the solution) can be influenced by adjusting the epistemic uncertainty term $\left(\sigma_R^2\right)$, so in these cases, σ_R^2 is set at a fixed value. In case 3, σ_R^2 is set low $\left(1.0 \times 10^{-5}\right)$ and the restricted maximum likelihood algorithm is given the freedom to estimate it. This setup illustrates the best achievable fit that one might achieve given the specific observation set provided without regard for overfitting. In cases 5 and 6, estimates are made with specification of

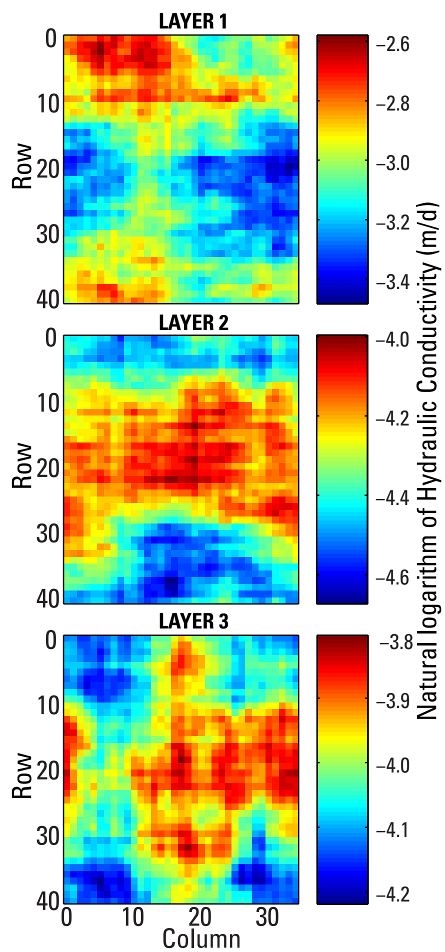

Figure 6.1. True synthetic hydraulic conductivity field for each layer in the three layer example application. Values are shown in natural logarithm space to make the differences more visible.

Table 6.1. Summary of the five cases investigated. The table shows which structural parameters were estimated and fixed, and also indicates anisotropy when used.

		Scenario	Case 1	Case 2	Case 3	Case 4	Case 5
		Initial σ_R^2	1.00E-01	1.00E-02	1.00E-05	1.00E-04	1.00E-01
		Estimated σ_R^2	-	-	7.79E-08	1.18E-05	-
Prior Parameters	**Beta Association 1**	Initial θ	1.00E-05	1.00E-05	1.00E-05	1.00E-05	1.00E-05
		Estimated θ	2.46E-03	1.55E-02	1.25E-02	5.54E-03	3.61E-03
	Beta Association 2	Initial θ	1.00E-05	1.00E-05	1.00E-05	1.00E-05	1.00E-05
		Estimated θ	6.16E-03	2.47E-02	1.34E-02	3.19E-03	7.97E-03
	Beta Association 3	Initial θ	1.00E-05	1.00E-05	1.00E-05	1.00E-05	1.00E-05
		Estimated θ	2.46E-03	1.55E-02	1.21E-02	2.51E-03	7.73E-05
Anisotropy Parameters	**Beta Association 1**	horiz_angle	-	-	-	0.0	0.0
		horiz_ratio	-	-	-	100.0	100.0
		verical_ratio	-	-	-	1.0	1.0
	Beta Association 2	horiz_angle	-	-	-	0.0	0.0
		horiz_ratio	-	-	-	100.0	100.0
		verical_ratio	-	-	-	1.0	1.0
	Beta Association 3	horiz_angle	-	-	-	0.0	0.0
		horiz_ratio	-	-	-	100.0	100.0
		verical_ratio	-	-	-	1.0	1.0

anisotropy in the prior covariance. Inspection of the true parameter field in figure 6.1 suggests a possible correlation along the horizontal axis, indicative of a channel feature. In cases 5 and 6, therefore, an arbitrarily chosen ratio of 100 is applied with a rotation angle of zero. In case 4, like in case 3, σ_R^2 is estimated to achieve the best possible fit, whereas in Case 5, σ_R^2 is held constant at 1.0×10^{-1}.

Figures 6.2 and 6.3 show the estimated hydraulic conductivity field and squared differences between measured and observed head values, respectively, for case 1. In this case, meant to be conservative with respect to overfitting, the squared differences are smaller in magnitude than the specified value of σ_R^2 $\left(1.0 \times 10^{-1}\right)$ and very little roughness in the solution is required to achieve the level of fit desired.

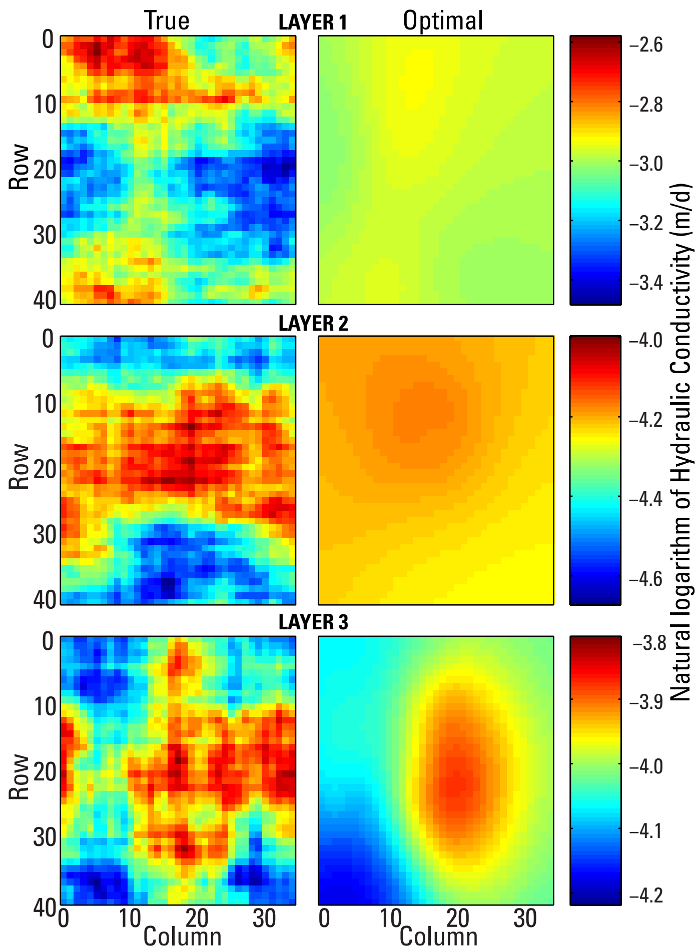

Figure 6.2. Case 1: Hydraulic conductivity fields estimated by using bgaPEST compared to the true, synthetic hydraulic conductivity field. σ_R^2 is held constant at 1.00×10^{-1}.

Figures 6.4 and 6.5 show the estimated hydraulic conductivity field and squared differences between measured and observed head values, respectively, for case 2. In this case, the specified value of σ_R^2 $\left(1.0 \times 10^{-2}\right)$ is lower than in case 1 and, accordingly, the squared head differences are lower, and more structure (roughness) is observed in the parameters, as expected. Note that, in this case, even with very low residuals, the parameter fields estimated are a smoothed representation of the "truth."

Figures 6.6 and 6.7 show the estimated hydraulic conductivity field and squared differences between measured and observed head values, respectively, for case 3. In this case, the value of σ_R^2 is estimated by the restricted maximum likelihood value algorithm. The head values match perfectly to machine precision, and the roughness of the field is the greatest of cases 1 through 3, as expected. The major features of the "true" hydraulic conductivity field are reproduced by this solution although they are smoothed, somewhat, as expected. Importantly, although the highest hydraulic conductivity values in layer 2 are slightly offset to the west, no artifacts are introduced that would be considered spurious in this solution.

Figures 6.8 and 6.9 show the estimated hydraulic conductivity field and squared differences between measured and observed head values, respectively, for sase 5. In this case, the value of σ_R^2 is set very low $\left(1.0 \times 10^{-4}\right)$ to attempt to achieve excellent fit while introducing anisotropy with the principal direction aligned with the horizontal axis. In layer 1, a somewhat spurious artifact is visible in the form of a high hydraulic conductivity zone near the middle of the field. The head targets almost match within machine

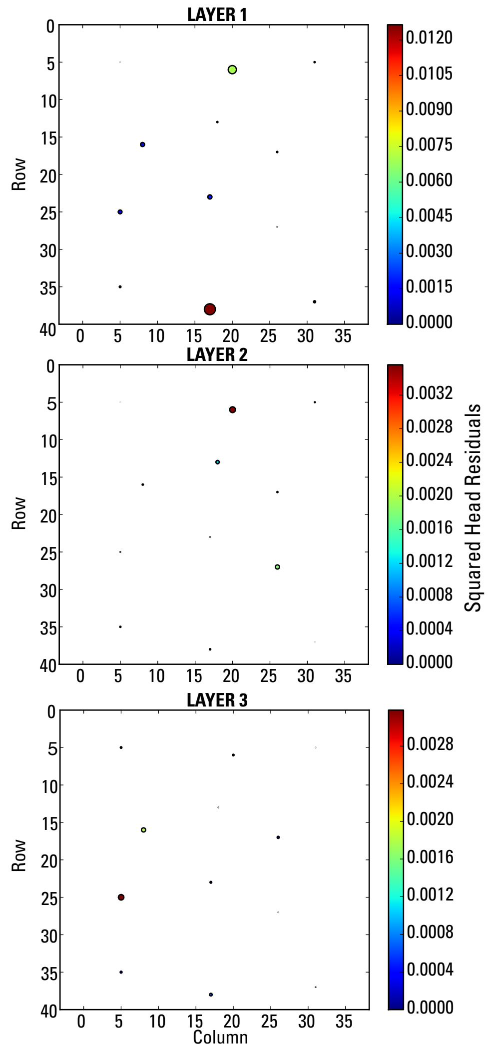

Figure 6.3. Case 1: Squared differences between modeled and "true" head values. Symbol size qualitatively indicates magnitude, and color scale quantifies magnitude. Locations of the circles indicate observation location in the model domain in plan view. σ_R^2 is held constant at 1.00×10^{-1}.

precision, however, and all other features are reasonable. This highlights the fact that, within a single beta association, if anisotropy is used, *all* features estimated will roughly correspond to that framework so, in a Bayesian sense, the answer is *conditional* on the prior assumption that the anisotropy is an appropriate general characteristic shape of the parameter field. Such assumptions must be made cautiously.

Figures 6.10 and 6.11 show the estimated hydraulic conductivity field and squared differences between measured and observed head values, respectively, for case 5. In this case, the value of σ_R^2 is set at a the same value as case 1 $\left(1.0 \times 10^{-1}\right)$ to compare a solution with and without anisotropy assumed. Because anisotropy is a reasonable characteristic of the "true" field in this case, better fits are achieved (nearly an order of magnitude lower residuals) and the general pattern of the parameter field is better in case 5 with anisotropy than in case 1 without anisotropy. This highlights the power that anisotropy can bring to a parameter estimation problem when it is appropriate even when σ_R^2 is set conservatively to avoid overfitting. As discussed above, however, this anisotropy will, in a sense, force the solution to conform to such a shape, so it's use should be approached with caution.

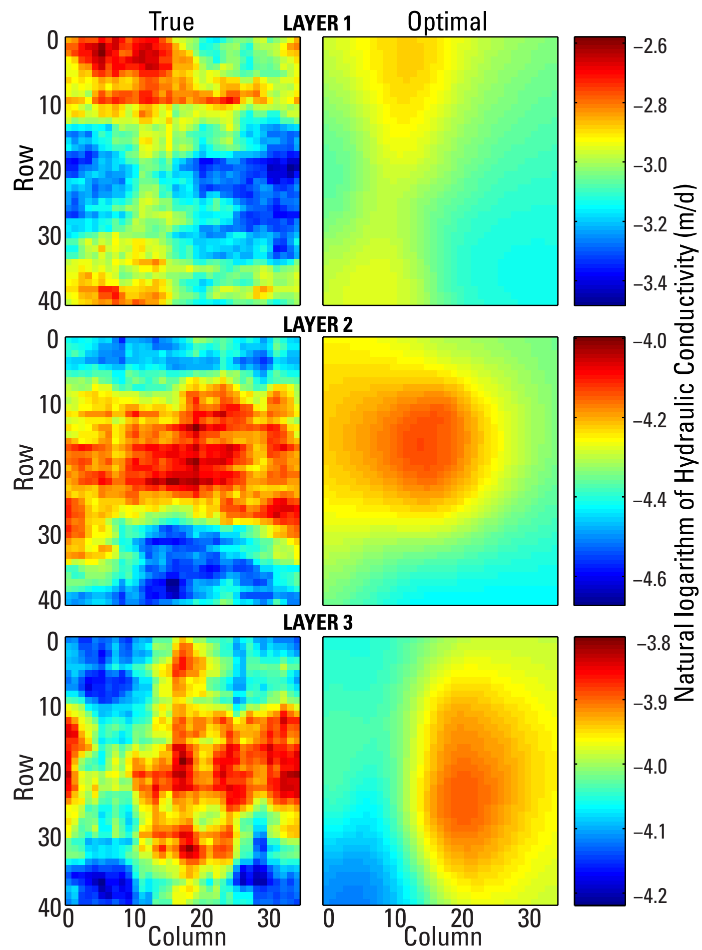

Figure 6.4. Case 2: Hydraulic conductivity fields estimated by using bgaPEST compared to the true, synthetic hydraulic conductivity field. σ_R^2 is held constant at 1.00×10^{-2}.

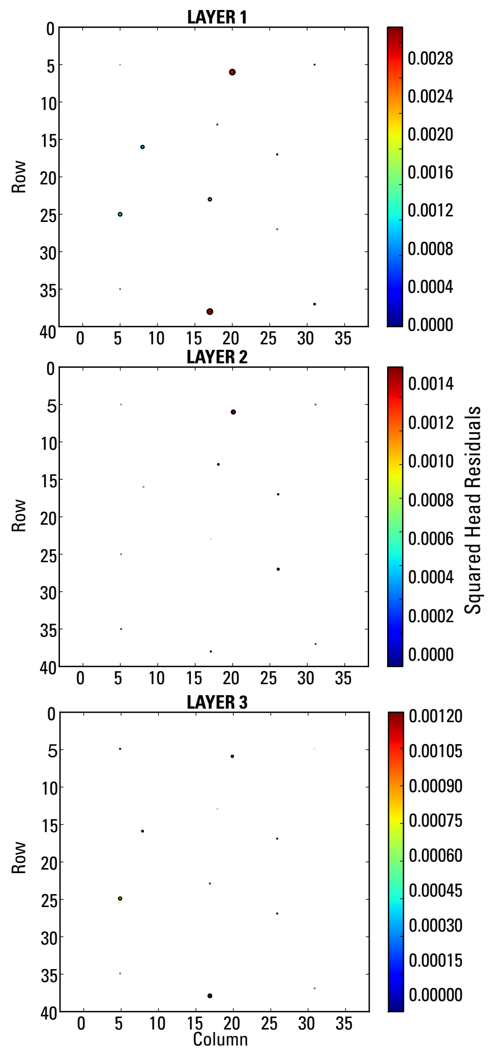

Figure 6.5. Case 2: Squared differences between modeled and "true" head values. Symbol size qualitatively indicates magnitude, and color scale quantifies magnitude. Locations of the circles indicate observation location in the model domain in plan view. σ_R^2 is held constant at 1.00×10^{-2}.

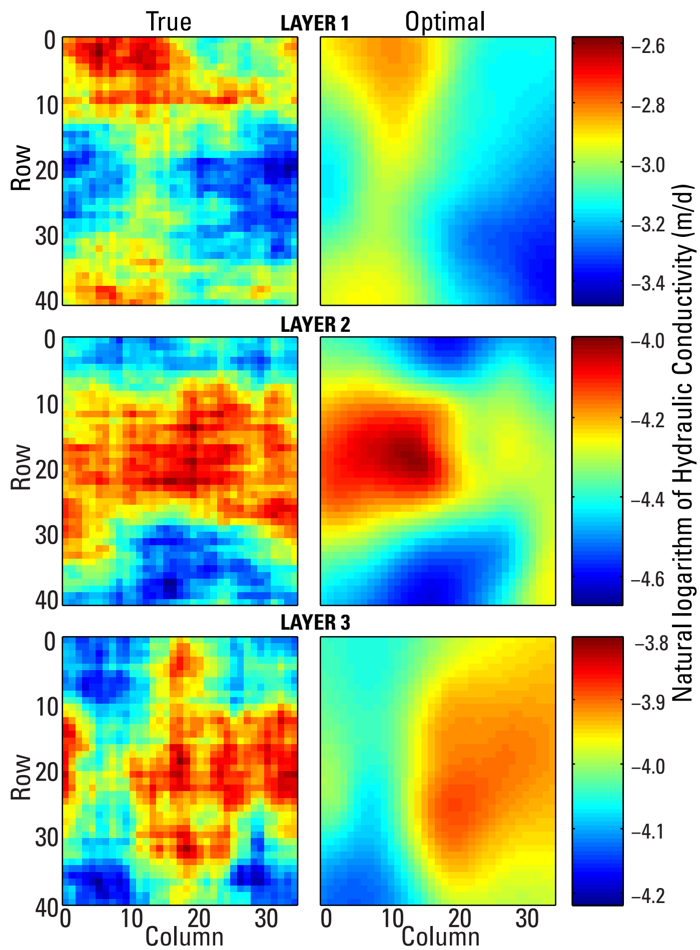

Figure 6.6. Case 3: Hydraulic conductivity fields estimated by using bgaPEST compared to the true, synthetic hydraulic conductivity field. σ_R^2 is initially 1.00×10^{-5} and estimated by bgaPEST at an optimal value of 7.79×10^{-8}.

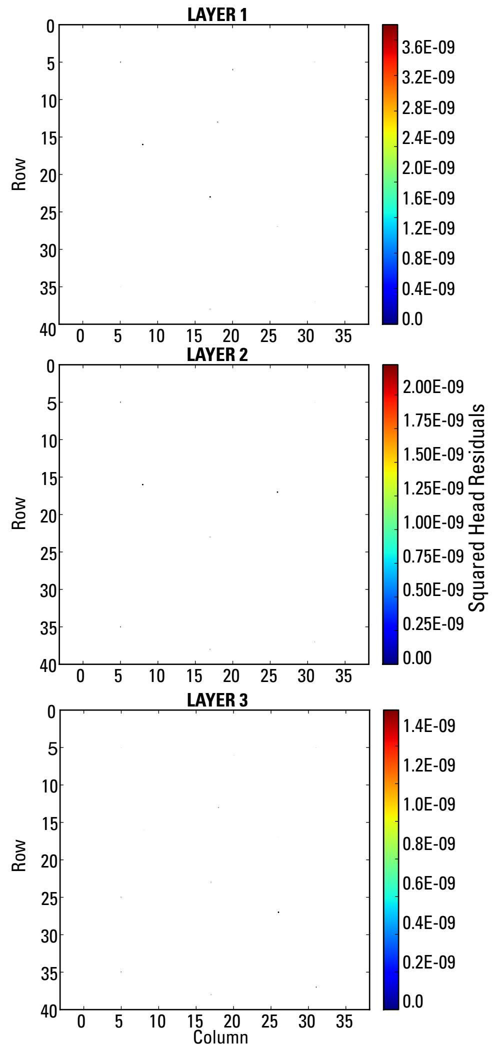

Figure 6.7. Case 3: Squared differences between modeled and "true" head values. Symbol size qualitatively indicates magnitude, and color scale quantifies magnitude. Locations of the circles indicate observation location in the model domain in plan view. σ_R^2 is initially 1.00×10^{-5} and estimated by bgaPEST at an optimal value of 7.79×10^{-8}.

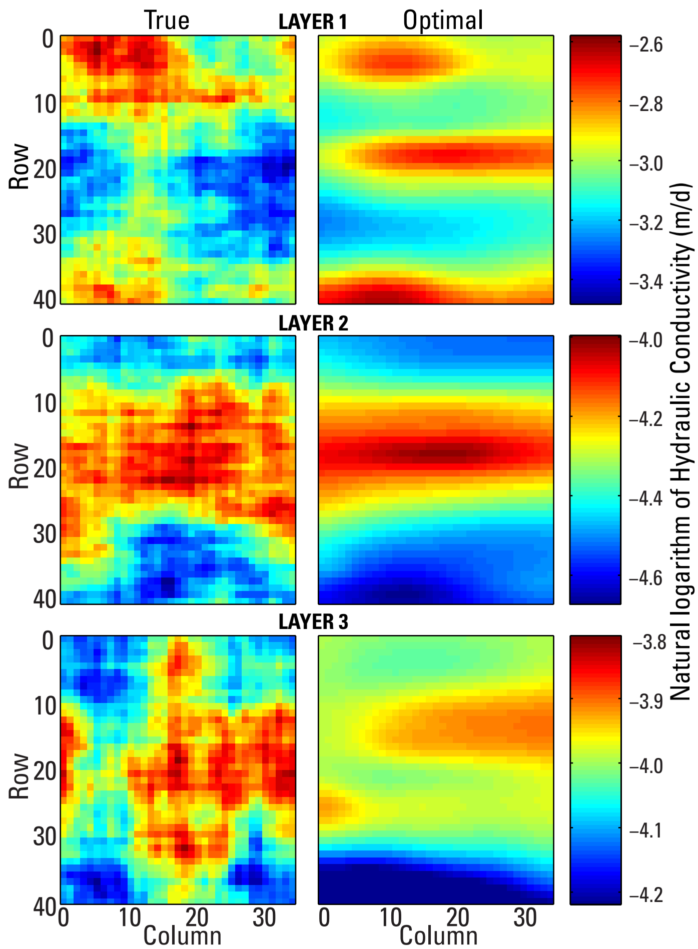

Figure 6.8. Case 4: Hydraulic conductivity fields estimated by using bgaPEST compared to the true, synthetic hydraulic conductivity field. σ_R^2 is initially 1.00×10^{-4} and estimated by bgaPEST at an optimal value of 1.18×10^{-5}. Parameter anisotropy also invoked as described in Table 6.1.

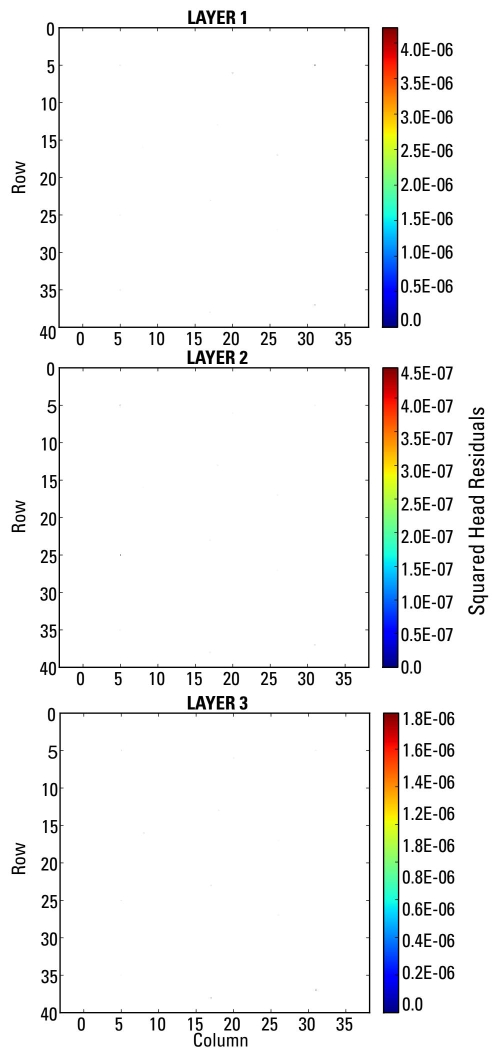

Figure 6.9. Case 4: Squared differences between modeled and “true” head values. Symbol size qualitatively indicates magnitude, and color scale quantifies magnitude. Locations of the circles indicate observation location in the model domain in plan view. σ_R^2 is initially 1.00×10^{-4} and estimated by bgaPEST at an optimal value of 1.18×10^{-5}. Parameter anisotropy also invoked as described in Table 6.1.

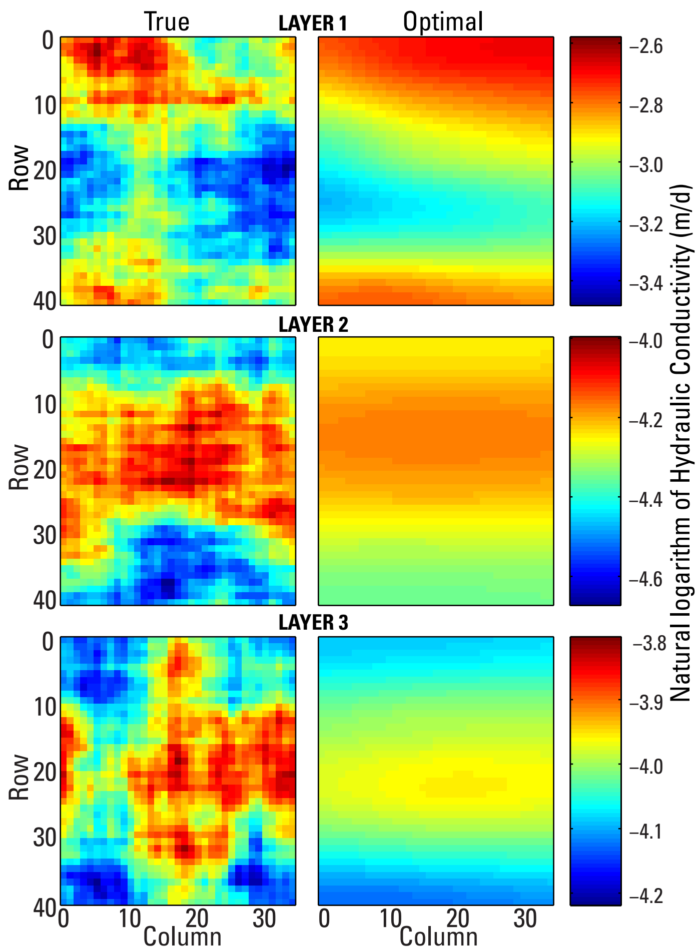

Figure 6.10. Case 5: Hydraulic conductivity fields estimated by using bgaPEST compared to the true, synthetic hydraulic conductivity field. σ_R^2 is held constant at 1.00×10^{-1}. Parameter anisotropy also invoked as described in Table 6.1.

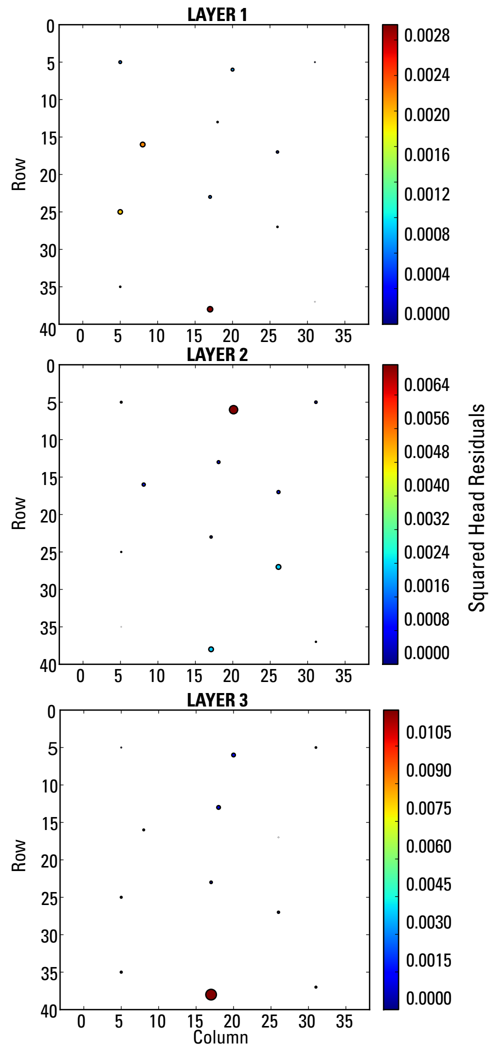

Figure 6.11. Case 5: Squared differences between modeled and "true" head values. Symbol size qualitatively indicates magnitude, and color scale quantifies magnitude. Locations of the circles indicate observation location in the model domain in plan view. σ_R^2 is held constant at 1.00×10^{-1}. Parameter anisotropy also invoked as described in Table 6.1.